REPORT DOCUMENTATION PAGE

AFRL-SR-AR-TR-03-

0199

22 2003

1. AGENCY USE ONLY (Leave blank)	2. REPORT DATE	3. REPORT TY
	4/18/2003	FINAL TECHNICAL RPT 1 MAR 1999 to 31 MAR 2002

4. TITLE AND SUBTITLE

INTERFACIAL ATOMIC STRUCTURE, SEGREGATION AND STRENGTH OF POLYSYNTHETICALLY-TWINNED TiAl

5. FUNDING NUMBERS

F49620-99-1-0167

6. AUTHOR(S)

David E. Luzzi

7. PERFORMING ORGANIZATION NAME(S) AND ADDRESS(ES)

University of Pennsylvania, Office of
Research Services, Rm. P-221
3451 Walnut Street
Philadelphia, PA 19104

8. PERFORMING ORGANIZATION REPORT NUMBER

533718

9. SPONSORING / MONITORING AGENCY NAME(S) AND ADDRESS(ES)

AFOSR/NA, 801 N. Randolph Street,
Room 732, Arlington, VA 22203-1977

ONRRO Chicago, 536 South Clark St.
Rm. 208, Chicago, IL 60605-1588

10. SPONSORING / MONITORING AGENCY REPORT NUMBER

11. SUPPLEMENTARY NOTES

12a. DISTRIBUTION / AVAILABILITY STATEMENT

Unlimited

20030612 027

13. ABSTRACT *(Maximum 200 Words)*

Polysynthetically-twinned titanium aluminide (PST-TiAl), a fully lamellar γ–TiAl + α_2-Ti_3Al dual-phase alloy, is under evaluation for applications in rotary components in aircraft and automobile industries due to its high specific strength, and a high strength-retention capability at elevated-temperatures. However, the low ductility at room- to mid-high temperatures of the material hinders its application. Additions of certain tertiary elements to the binary TiAl system appear to improve the ductility at room- to mid-high temperatures, thus a balance among strength, ductility, and fracture toughness can be expected. In this article, segregation of tertiary elements to the lamellar interfaces is investigated. Single crystals of a TiAl with 0.6% atomic percentage tertiary additions are grown by an optical float-zone method. Segregation to the lamellar interfaces and the microstructure of the interfaces are investigated. Structures of the lamellar interfaces are characterized, and microchemistry and distribution habits of these elements along the $\gamma+\alpha_2$ lamellar boundaries as well as the γ-γ lamellar and domain boundaries are analyzed.

14. SUBJECT TERMS

Polysynthetically-twinned titanium aluminide

15. NUMBER OF PAGES

11

16. PRICE CODE

17. SECURITY CLASSIFICATION OF REPORT	18. SECURITY CLASSIFICATION OF THIS PAGE	19. SECURITY CLASSIFICATION OF ABSTRACT	20. LIMITATION OF ABSTRACT
UNCLASSIFIED	UNCLASSIFIED	UNCLASSIFIED	UL

INTERFACIAL ATOMIC STRUCTURE, SEGREGATION AND STRENGTH OF POLYSYNTHETICALLY-TWINNED TiAl

F49620-99-1-0167

David E. Luzzi
Department of Materials Sciences and Engineering, University of Pennsylvania,
3231 Walnut Street, Philadelphia, PA 19104-6272

Abstract

Polysynthetically-twinned titanium aluminide (PST-TiAl), a fully lamellar γ–TiAl + α_2-Ti_3Al dual-phase alloy, is under evaluation for applications in rotary components in aircraft and automobile industries due to its high specific strength, and a high strength-retention capability at elevated-temperatures. However, the low ductility at room- to mid-high temperatures of the material hinders its application. Additions of certain tertiary elements to the binary TiAl system appear to improve the ductility at room- to mid-high temperatures, thus a balance among strength, ductility, and fracture toughness can be expected. In this article, segregation of tertiary elements to the lamellar interfaces is investigated. Single crystals of a TiAl with 0.6% atomic percentage tertiary additions are grown by an optical float-zone method. Segregation to the lamellar interfaces and the microstructure of the interfaces are investigated. Structures of the lamellar interfaces are characterized, and microchemistry and distribution habits of these elements along the γ+α_2 lamellar boundaries as well as the γ-γ lamellar and domain boundaries are analyzed.

Research Objective

The objective of this research program is to understand the relationships between structural, thermodynamic and mechanical properties of TiAl through studies of the atomic structure, diffusion, segregation and strength at γ-γ and α_2-γ interfaces in polysynthetically twinned (PST) TiAl with and without ternary alloying additions.

Introduction

Polysynthetically-twinned titanium aluminide (PST-TiAl) single crystals comprised of lamellar TiAl and Ti_3Al provide the opportunity to distinguish the behavior of the two phases and the different lamellar interfaces. The near coherency of the lamellar interfaces allows direct imaging of the interface atomic structure with the atomic-level flatness enabling high-resolution studies of the segregation of tertiary elements. With precise crystal lattice relationships maintained over macroscopic distances, crystal orientation effects on properties can be studied. At the present time, little is known about the segregation properties of the different lamellar interfaces in TiAl alloys, and almost nothing is known about the effects of the segregation on the strength and deformation behavior of these lamellar interfaces.

Experimental details

Both binary and ternary alloys were prepared by arc-melting using a non-consumable tungsten electrode. One of the elements Mn, Fe, Co, Ni, Cu, Mo, W or Ta was added to each ternary alloy. The nominal composition of the binary alloy was Ti-49.3 at.%-Al. Tertiary additions of 0.6 at.% were used to facilitate the growth of the PST single crystals. This addition replaced the Ti and Al in equal measure producing ternary alloy compositions of Ti-49 at.% Al-.6 at.% X.

The PST crystals were grown from master ingots using an ASGAL FZ-SS35W optical floating-zone furnace at a growth rate of less than 5 mm/h under an Ar gas flow. Growth rates as slow as 2.5 mm/h were necessary in order to obtain PST single crystals of some of the ternary alloys. All crystals have a lamellar structure. The crystals contain about 5% of the Ti_3Al α_2 phase in a matrix of lamellar TiAl γ phase.

Crystal orientations were determined using a Back-Laue X-ray diffractometer, and sometimes, reconfirmed by RIGAKU x-ray diffraction spectra to identify the required preferred crystal orientations. Specimens with dimensions 5x5x0.5 mm^3 were machined from the oriented PST crystals by an electric spark discharge machine. The lamellar structure is composed of γ TiAl and α_2 Ti_3Al lamellae with orientation relationships of $\{111\}_\gamma \| (0001)_{\alpha 2}$ and $\langle 110]_\gamma \| \langle 1120 \rangle_{\alpha 2}$; the lamellar boundaries are parallel to $(111)\gamma$. Slices were machined with the normal to the thin dimension parallel to the γ <111>, <110> and <112> directions, i.e., parallel or normal to the lamellar boundaries. Mechanically polished TEM 3mm-ϕ discs were machined using an ultrasonic disc cutter from the as-polished PST-TiAl samples. TEM thin foils were prepared by electropolishing to perforation using a Tenupol-3 twin-jet electropolisher at 20 V and –30 °C with a solution consisting of 6% perchloric acid and 35% butyl alcohol in 59% methanol. The foils were examined in a Philips 420 TEM operating at 120kV to determine quality and to examine crystallographic and microstructural features. A JEOL-2010F field emission scanning TEM (FE-STEM) operating at 200 kV was used for advanced observations and chemical analysis. A Princeton Gamma Tech energy dispersive x-ray fluorescence spectrometer (EDS) equipped with a 60mm^2 SiLi detector was used to determine the distribution of Ti, Al and the ternary element additions in the specimens.

For diffusion-bonding experiments, slices of the PST crystals were mechanically and electrolytically polished in a solution of 6 vol.% perchloric acid (70%), 35 vol.% n-butyl alcohol and 59 vol.% methanol prior to diffusion bonding. Bulk Ti (99.999%) specimens were mechanically polished in parallel using an Allied High Tech MultiPrep polisher to an ultimate finish of 1200-grit. Diffusion couples of PST Ti-Al and Ti were produced by diffusion bonding in a graphite high vacuum furnace at 600°C for two hours. No extra mechanical stress was applied to the material during diffusion bonding except that from the thermal expansion of the graphite rams. A sketch of the diffusion couple is shown in Figure 1. Cross-sections of the as-bonded diffusion couples were cut perpendicular to both the bonding plane and the lamellar interfaces of the PST crystal, i.e. parallel to the front surface in Figure 1, and were observed with a JEOL 6400 scanning electron microscope (SEM) operated at 15 kV. The as-bonded diffusion couples were subjected to diffusion anneals in the same furnace at temperatures 650, 700, 750, 800, 850 and 900°C for various times. Transmission electron microscopy (TEM) specimens were cut from the annealed diffusion couples using a Strata DB 235 dual beam focused ion beam

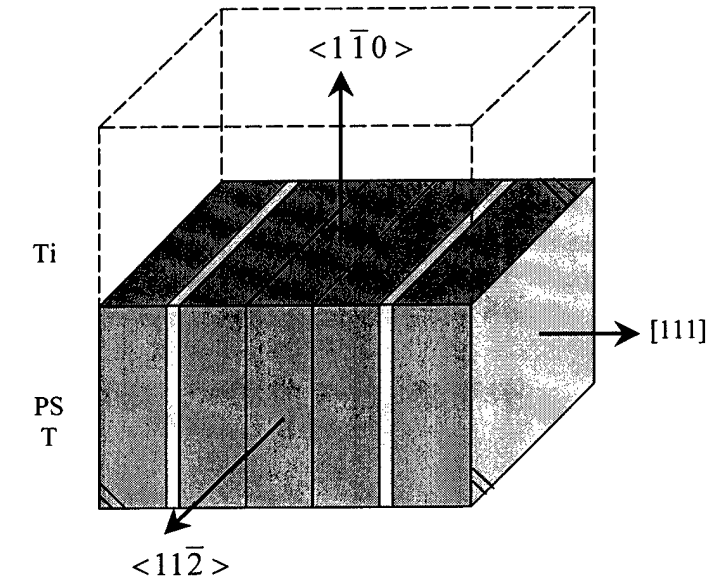

Figure 1. Schematic of Ti / PST-TiAl diffusion couple.

(FIB) system at Lehigh University. Thin foils for TEM analysis were prepared with foil normals near to <11 $\bar{2}$>, [111] and <110>. Most observations, including all in this paper, were made on foils with the <11 $\bar{2}$> orientation. SEM samples had the same normal, i.e. <11 $\bar{2}$>. TEM specimens were examined in a JEOL 2010F TEM operated at 200 kV. The diffusion experiments were partially funded by the NSF.

Results and discussions

Ternary alloying of Ti-Al at the compositions of this study is a counter-indicator for successful single crystal growth. Nevertheless, with careful attention to shape of seed and feed rods, alignment, cleanliness of the material and the surrounding quartz tube, and a high-purity, oxygen-gettered inert flowing gas environment, single crystals were obtained for all ternary systems in this paper. In some systems, it was necessary to reduce the growth rate at the start of the growth process, with a gradual increase after the first crystal was formed. Frequent monitoring of the power level of the furnace and careful adjustment was necessary to achieve successful growth. Patience is a valuable trait.

In Figure 2, bright-field and corresponding g-3g weak-beam TEM images of the microstructure of the ternary alloy Ti-Al-Mo are shown. The electron beam is oriented parallel to the lamellar

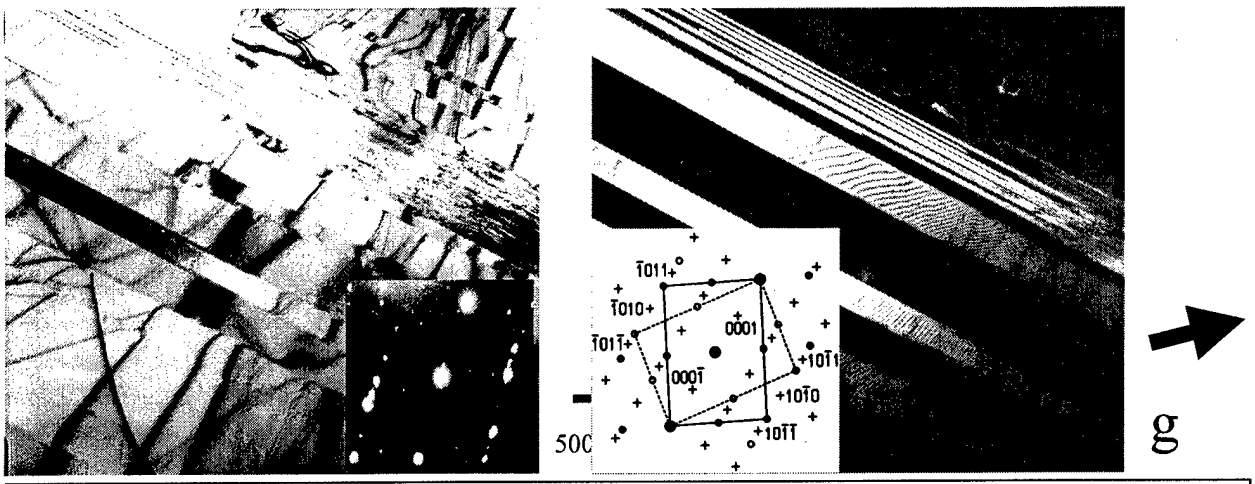

Figure 2. A bright field image (left) and a g-3g weak-beam image (right) for a PST-TiAl+Mo single crystal showing the hcp α_2 (Ti_3Al) lamellae and the twin-related lamellar boundaries of fct γ–γ (TiAl), beam // [1-10].

interfaces along the $[1\bar{1}0]_\gamma$ crystal direction. The bright field and weak-beam show complementary contrast that differentiates the hcp α_2 (Ti_3Al) lamellae from the twin-related lamellae of the fct γ–γ (TiAl). The superlattice diffraction pattern from the region is an overlapping of those due to the twin-related fct γ and hcp α_2 phases; the diffraction spots of the hcp DO_{19} lattice are marked as +. It is apparent that PST-TiAl still preserves the lamellar structure with 0.6 at. % addition of Mo. It is known that Mo will segregate to γ–γ interfaces [1]. The atomic number of Mo is relatively high compared to Ti and Al (42 versus 22 and 13, respectively). This is important for the HR-TEM experiments in which the differences in atomic numbers facilitate the determination of the interface atomic structure. However, the segregation of Mo is at the same time very interesting from the perspective of general theoretical comprehension of driving forces for segregations. Its atomic size is smaller than that of Ti and Al. Therefore, its segregation to interfaces cannot be explained by the standard model in which the segregation propensity is controlled by the atomic size and the increase of the atomic volume at the interface makes the segregation favorable. This is a topic that is worthy of further investigation.

TEM micrographs of the lamellar interfaces taken at orientations away from the edge-on configuration were used to study the dislocation structure at the interfaces. This analysis showed the existence of arrays of dislocations in the ternary alloys. Analysis of these dislocations indicated that they are screw dislocations. This result is consistent with the result of Kad and Hazzledine (1992) who analyzed the misfit dislocation arrays in binary alloys by weak beam microscopy and concluded that they are composed solely of screw dislocations [2]. These misfit dislocations could function as possible preferred sites for interfacial segregation.

Figures 3 and 4 show FE-STEM results from the ternary Ti-Al-W system. In Figure 3, a set of elemental distributions (Ti, Al, W, and C, N, and O) obtained using STEM EDXS chemical mapping in a lamella region is shown. The sample is a single crystal of TiAl+W, (Al 49.0% + W 0.6 % at.). The image at the bottom left is a STEM bright field image that should be dark in the regions of higher atomic number. This is confirmed by comparing the elemental maps of Ti and Al, which show complementary contrast modulation differentiating the lamellae of α_2-Ti_3Al and γ–TiAl. The region of the specimen was chosen to contain similar amounts of each phase. Maps of C, N, and O indicate overall low levels of contamination consistent with surface adsorption; the small evidence of contrast modulation in these maps is due to their proximity to the low energy peak of Ti. In contrast, the W map indicates a strong segregation of W to the Ti_3Al phase.

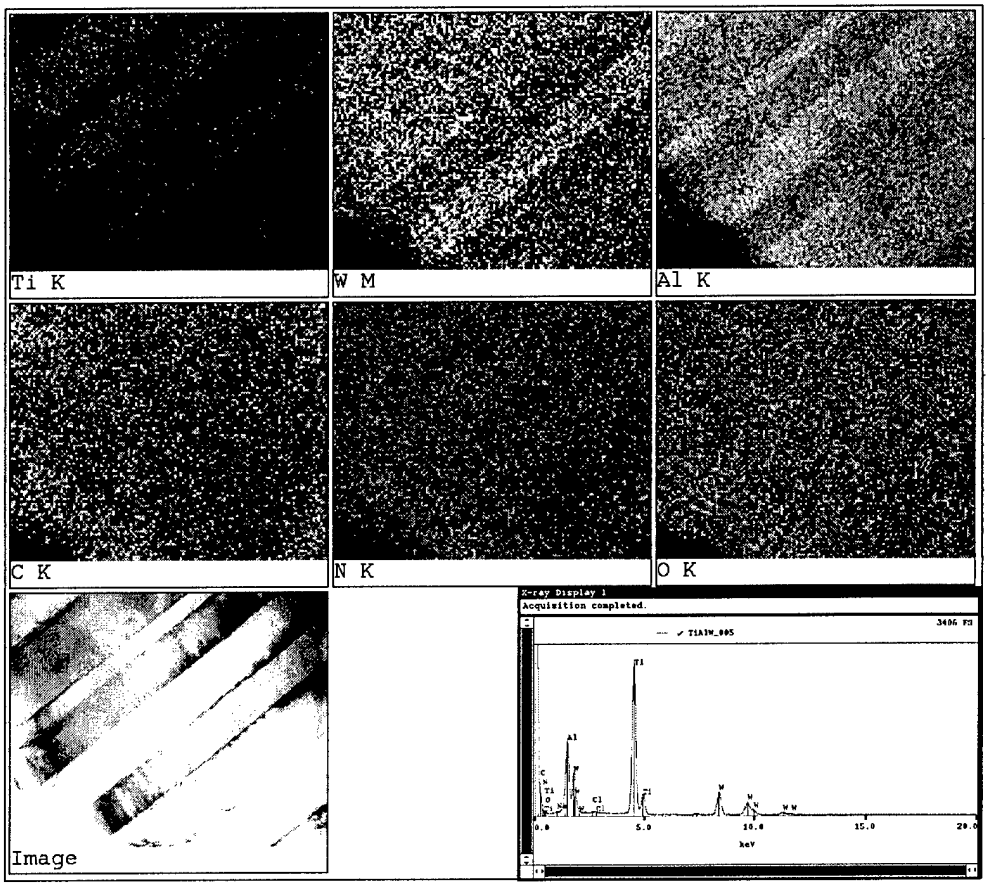

Figure 3. Elemental distributions (Ti, Al, W, and C, N, and O) by STEM EDXS Elemental Mapping in a lamella region (a single crystal of TiAl+W, Ti 50.4% + Al 49.0% + W 0.6 % at.)

In Figure 4, the strong segregation property of W is revealed in more detail. W concentrates in α_2-Ti_3Al lamellae and an accumulation of W is seen at γ-TiAl lamellar boundaries. At the lower right of the figures, a precipitate is seen to have formed along a γ/γ lamellar boundary. This boundary and the precipitate are seen to be rich in W and Ti with the precipitate showing strong W contrast. Thus it appears that excess W has segregated to a γ/γ lamellar boundary, perhaps forming a thin layer of the α_2 phase. On the same boundary, a W-rich precipitate has formed. The structure of these boundaries and precipitates will be addressed in the next phase of the research.

Ternary W additions are known to provide the most significant increase in oxidation resistance and strength[3] and to improve creep resistance[4, 5], but also to lower room-temperature ductility[5] in polycrystalline TiAl materials. Moreover, the brittle-ductile transition (BDT) observed at ~650°C for most near γ-TiAl compositions is much less pronounced when W is present[5, 6], possibly because W solute impedes elevated temperature dislocation movement[6]. Consequently, TiAl+W exhibits lower ductility at elevated temperature than other near γ-TiAl compositions. For the PST-TiAl under current investigations with a near stoichiometric composition, 95 % of the lamellae are TiAl while 5 % are Ti_3Al. Even if the solubility of W is higher in Ti_3Al than in

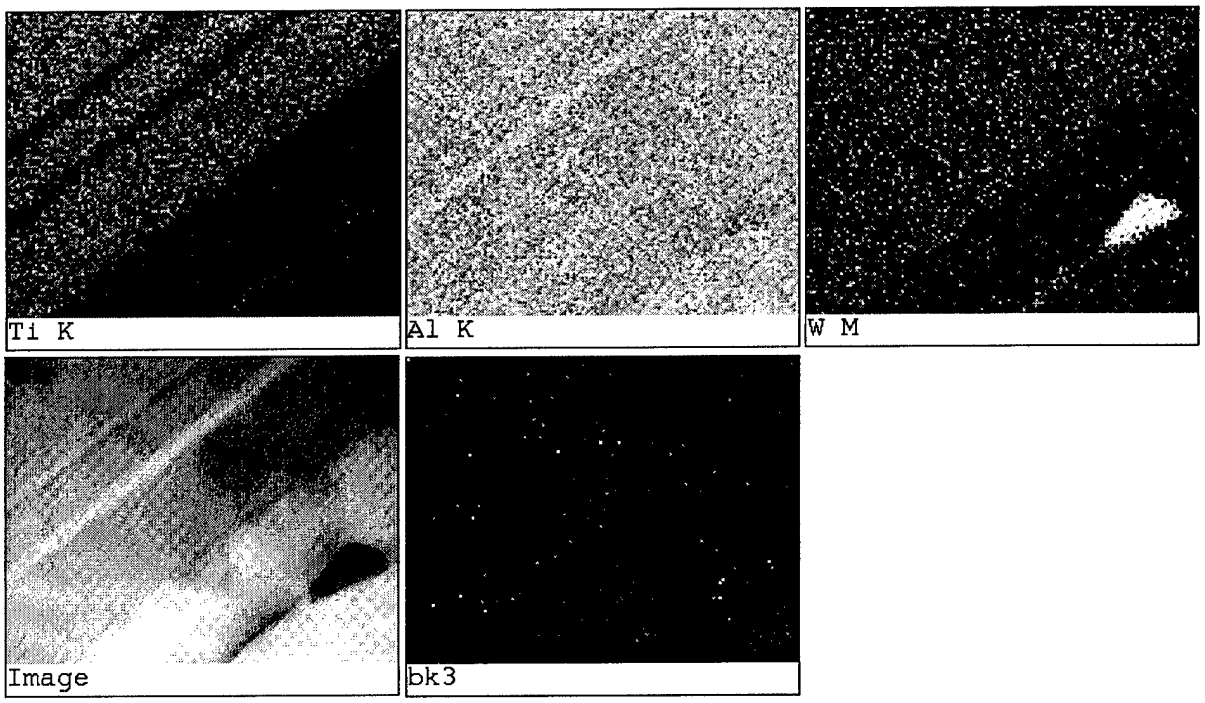

Figure 4. Distribution of W in α_2-Ti_3Al lamellae and accumulation of W at the interface of γ-TiAl (STEM EDXS for a single crystal of Ti 50.4% + Al 49.0% + W 0.6% at.)

TiAl, the small amount of W that is beyond the solubility limit of W in Ti_3Al could preferably segregate on the TiAl-TiAl boundaries, accumulate and then precipitate along the boundaries. These precipitates may serve to impede the processes, such as twinning and dislocation glide, that contribute to ductility in these alloys. In the other ternary systems studied, it was found that Ta was uniformly distributed in both the Ti_3Al phase and in the TiAl phase. Similarly, STEM XEDS mappings on TiAl with Mo displayed a similar trend, with some segregation of the Mo to the lamellar boundaries. For the case of Cu, it was found that the distribution of Cu is quite different from the others studied in the paper. Cu was found to be rich in regions coincident with excess Ti. However, at the same locations, Al was found to be significantly depleted, much below the level expected in Ti_3Al. It is possible that the Cu may react with Ti to form an intermetallic compound, of which there are several with high heats of formation within the Cu-Ti alloy system. Existing mechanical testing data indicate that 1 at% Cu additions slightly improves the strength and ductility of polycrystalline TiAl at 873 and 1073K, but at higher concentrations (2-3 at.%), decreases the fracture strength and strain additions. This was reported to be due to embrittlement due to a second phase and grain coarsening[7].

In diffusion couples of Ti/PST Ti-Al, a reaction layer or reaction zone (RZ) with wavy contour in the PST Ti-Al side emerges at the bonding interface after annealing and its thickness increases with annealing time. Electron diffraction patterns in TEM have verified that it is the α_2-Ti_3Al phase, which follows from the equilibrium phase diagram. To elucidate the growth kinetics of the reaction layer, SEM observations and measurements on back scattered electron images were carried out on the bulk diffusion couples after each anneal. Figure 5 shows a typical SEM back scattered electron image of a diffusion couple after an anneal at 650°C for eight

hours. The upper white part is the polycrystalline Ti and the lower lamellar structure is the PST crystal, with the gray vertical thin laths the α_2-Ti_3Al lamellae and the majority dark lamellae the γ-TiAl phase. The light gray layer between the Ti and the PST lamellae is the so-called RZ. Several interesting features are present in this image. First, the α_2-lamellae tend to group with some fine γ lamellae. Second, the RZ exhibits a clear contrast difference with both phases of the PST Ti-Al, indicating an abrupt composition change across the RZ/PST interface. Third, the penetration depth of the RZ into the γ lamellae is in general smaller than that into the α_2 lamellae.

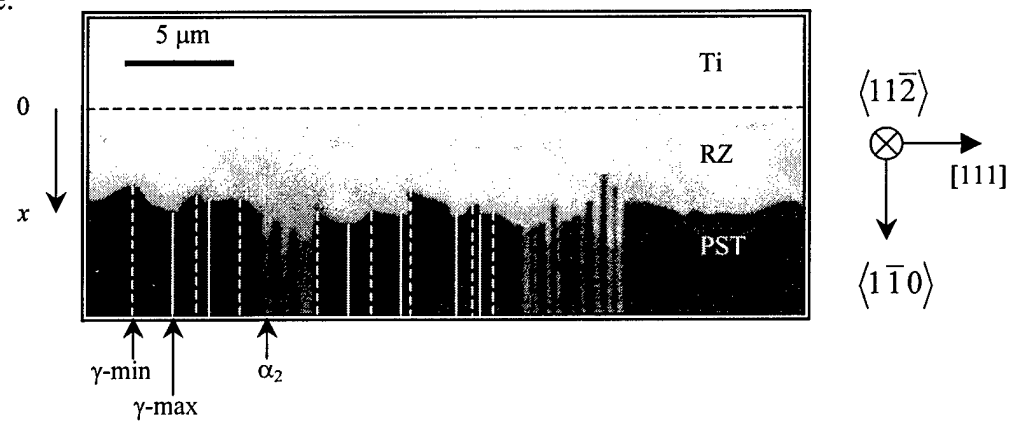

Figure 5. Illustration of the measurements of the RZ thickness from back scattered electron images of PST-Ti diffusion couple annealed at 650°C for 8 hours after bonding.

The clear contrast difference in the SEM back-scattered electron images between the RZ and the PST crystal allows a direct measurement of the thickness of the RZ. A series of SEM back-scattered electron images were recorded over a continuous region to form a map of each diffusion couple at each annealing condition. Since the RZ/Ti interface is mostly straight, a line across the interface of the RZ and Ti through the images is drawn and regarded as the zero-thickness level of the RZ, as illustrated in figure 5. The thickness of the RZ, x, was measured at each point where the RZ exhibited local minima or maxima in thickness adjacent to the γ-TiAl lamellae, categorized as γ-min and γ-max, respectively. In order to obtain the net increase of x corresponding to each individual annealing period, the average RZ thickness of the as-bonded diffusion couples was subtracted from the measurements in the annealed diffusion couples. Hundreds of measurements were made and averaged for both categories. The growth of the reaction layer is then illustrated by plotting x^2 versus t at each temperature, as shown in figure 6. It is revealed that x increases parabolically with the annealing time t, which indicates that the growth of the α_2-Ti_3Al phase in the RZ is mainly diffusion-controlled at a macroscopic level.

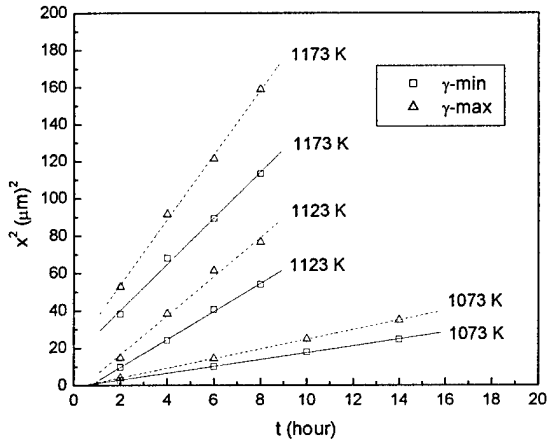

Figure 6. The parabolic growth of the reaction layer at various temperatures.

A typical TEM bright field image of a diffusion couple annealed at 1173 K for two hours is shown in figure 7(a), with the beam direction $\boldsymbol{B} = <1\,\bar{1}\,0>$ and the lamellar planes edge on. The interface types between the individual γ lamellae were determined by electron diffraction and are labeled — OT: ordinary twin, RF: rotational fault, PT: pseudo-twin. The penetration depth of the RZ into the α_2 lamella is much deeper than that in the γ lamellae, forming a well-like structure, which is consistent with the SEM observation. This deeper penetration in the mixed α_2 lath than in primary γ lamellae is mostly a result of mass balance. At the sidewalls of the well formed by the deeply penetrated RZ grain in the original mixed α_2 lath in figure 7(a), the interfaces between the RZ grain and the neighboring primary γ lamellae exhibit small angles with the lamellae, which is evidence of lateral lattice diffusion assisted RZ grain growth across the lamellae. It is obvious that the RZ grain growth across the lamellae is much less than the growth parallel to the lamellae. This is associated with the close-packed structure of the lamellar planes. The activation energy for the atoms crossing a close-packed plane is usually high. As a result, the RZ grain growth across the lamellae likely occurs through a ledge mechanism, which is consistent with the high resolution electron microscopy (HREM) observations. An enlarged image of the area enclosed by the rectangular box in figure 7(a) is shown as figure 7(b). As can be seen, the thick α_2 lamella consists of a set of finer lamellar structures. HREM was used to determine that the α_2 lamella is actually composed of much finer γ and α_2 lathes with thickness of 10-150 nm. This was a common observation for other thick α_2-Ti_3Al lamellae seen in other TEM specimens. The fine γ lamellae presumably formed by secondary precipitation within the thick α_2 lamellae during directional solidification of the PST crystal. For the ease of description, we shall denote this group of fine mixed phase lamellae as a "mixed α_2 lath".

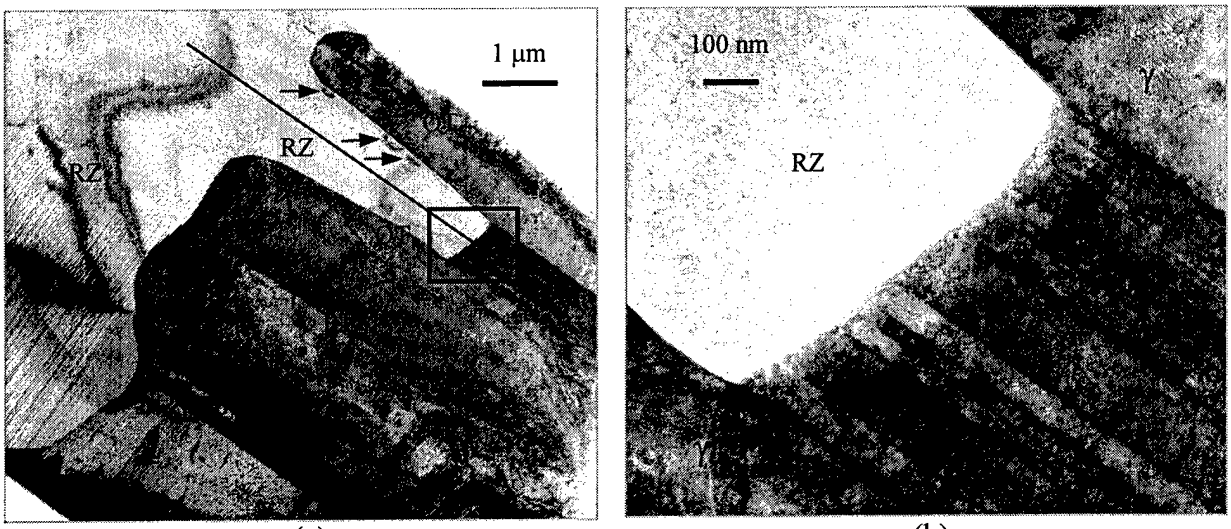

(a) (b)

Figure 7. Bright field TEM images of a diffusion couple that was annealed at 1173 K for two hours with $B = <1\,\bar{1}\,0>$ and the lamellar planes edge on. (b) is the magnified images of the area enclosed by the rectangular box in (a).

Concentration profiles were measured along the diffusion direction parallel to the lamellae with the lamellar planes edge on, from Ti, through the RZ, into both the mixed α_2 lath and the primary γ lamellae of the PST crystal, as indicated by the long arrow along the deeply penetrated RZ grain in figure 7(a). Figure 8 provides an example of the concentration profiles measured on the same specimen from the RZ into a secondary γ lamella in the mixed α_2 lath of the PST crystal and from the RZ into the two primary γ lamellae adjacent to this mixed α_2 lath. As illustrated by the schematic diagram of figure 8, the solid, dashed and dotted vertical lines in the concentration profiles indicate the interfaces between the RZ and secondary γ, primary $\gamma 1$ and primary $\gamma 2$ lamellae, respectively. As expected from the phase diagram, there are sharp discontinuities in composition across the RZ/γ interfaces. A plateau in composition in the RZ adjacent to the RZ/PST interface is also present and extends through most of the deeply penetrated well region, as observed in other specimens. In addition, it can be seen that although the penetration depth of the RZ into the primary γ lamellae and the mixed α_2 lath varies, the compositions at the same depth in the RZ are about the same regardless of their relative positions with respect to the lamellae.

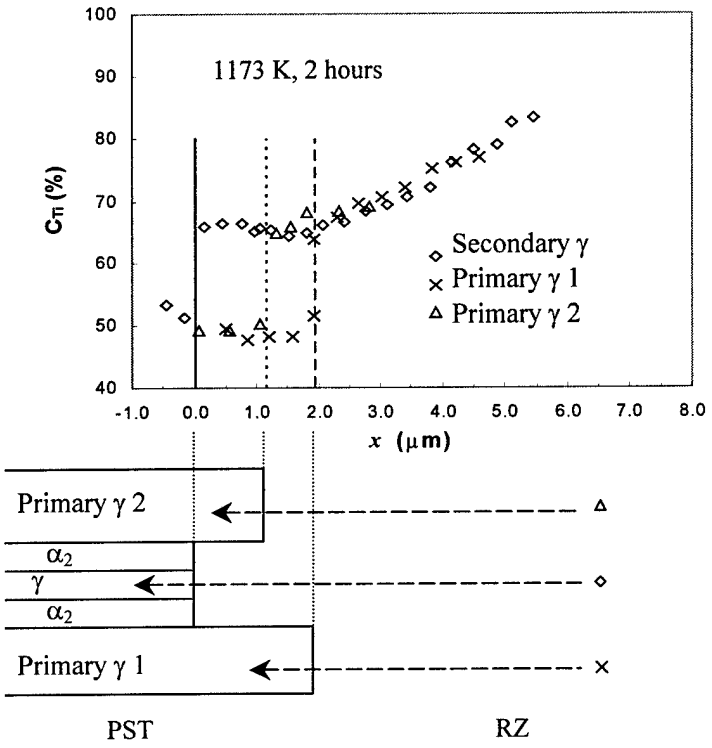

Figure 8. Concentration profiles from the RZ to a secondary γ lamella in the mixed α_2 lath and two primary γ lamellae of the diffusion couple annealed at 1173 K for two hours.

The discontinuity in composition at the RZ/α_2(PST) interface is an indication of the role of some extent of interface-controlled growth of the RZ. A possible explanation is that the RZ grain forms some arbitrary coherent or semicoherent boundary with the γ-TiAl lamellae while forming a high-angle GB with the α_2 lamellae. Therefore, the low mobility of the (semi)coherent boundary provides a barrier for the atoms to cross the boundary. The origins of the plateau in the diffusion profile are not quite clear. Since the plateau occurs in the deeply penetrated RZ well region, the following explanations are proposed. Increased interfacial energy and strain energy in the deeply penetrated well area that result from the phase transformation are proposed as the underlying cause for the plateau. The presence of this increased energy state is evident from the bend contours present in figure 7(a), marked by the small arrows, which are indications of the structural strain due to the incoherent RZ/(primary γ) interface at the sidewall of the well.

The interdiffusion coefficient is evaluated both independent of composition and as a function of composition. No significant concentration dependence of the interdiffusion coefficients is observed using Boltzmann-Matano analysis. The temperature dependence of the interdiffusion coefficients obeys the Arrhenius relationship with a pre-exponential factor of $D_0 = (7.56 \pm 7.14) \times 10^{-5}\ m^2/s$ and an activation enthalpy of $Q = \left(255.6^{+8.9}_{-8.3}\right) kJ/mol$.

REFERENCES

Personnel Supported

David E. Luzzi	Associate Professor, University of Pennsylvania
Wei Zhao	Postdoctoral Fellow, University of Pennsylvania
Ling Pan	Graduate Student, University of Pennsylvania

Publications

1. "Characterizations Of Lamellar Interfaces For a γ-Tial Alloy By An Analytical Scanning Transmission Electron Microscope", W. Zhao and D.E. Luzzi, in High-Temperature Ordered Intermetallic Alloys IX, eds. J.H. Schneibel, S. Hanada, K.J. Hemker, R.D. Noebe, G. Sauthoff, (MRS, 2001), Vol. 646.
2. "Characterizations of Lamellar Interfaces and Segregations in a PST-TiAl Intermetallic Alloy by an Analytical Scanning Transmission Electron Microscope", W. Zhao and D.E. Luzzi, in High-Temperature Ordered Intermetallic Alloys IX, eds. J.H. Schneibel, S. Hanada, K.J. Hemker, R.D. Noebe, G. Sauthoff, (MRS, 2001), Vol. 646.
3. "Microstructure Evolution in PST Ti-Al/Ti Diffusion Couples", L. Pan and D.E. Luzzi, Philos. Mag. (in press).
4. "Element Distributions in Ternary γ+α2 PST-TiAl+X (W, Ta, Mo, or Cu) Alloys Characterized by an Analytical STEM", Intermetallics (in preparation).
5. "Tungsten Partitioning Habits and Lamellar Interfacial Structures in a Ternary PST-TiAl+W Alloy Investigated by Analytical STEM and High-Resolution TEM", Mater. Sci. and Eng. (in preparation).

References

1 H. Inui, K. Kishida, M. Kobayashi, *et al.*, Philosophical Magazine A **74**, 451 (1996).

2 B. K. Kad and P. M. Hazzledine, Philosophical Magazine Letters **66**, 133 (1992).

3 P. Martin, (Wright Laboratory, 1991).

4 Y.-W. Kim, J of Metals **41**, 24 (1989).

5 P. L. Martin and H. A. Lipsitt, (Institute of Metals, London, 1990), p. 255.

6 J. Beddoes, L. Zhao, and W. Wallace, , edited by F. H. Froes, W. Wallace, R. A. Cull and E. Struckholt, 1992), p. M657.

7 T. Kawabata, H. Fukai, and O. Izumi, Acta. Mater. **46**, 2185 (1998).